

# Application of the Wide-Field Shadowgraph Technique to Helicopters in Forward Flight



Jeffrey S. Light  
Research Engineer  
NASA Ames Research Center  
Moffett Field, Calif.



Alexandra A. Swanson  
Research Engineer  
Sterling Federal Systems  
Moffett Field, Calif.



Thomas R. Norman  
Research Engineer  
NASA Ames Research Center  
Moffett Field, Calif.

A test was conducted to examine the feasibility of using the wide-field shadowgraph method for visualizing the wake of a small-scale helicopter rotor in forward flight. A wide range of test conditions was examined, including thrust and forward speed variations. Shadowgraphs from the side and top of the rotor were obtained. The visibility of the tip vortices using the shadowgraph method was documented for advance ratios up to 0.175. It was demonstrated that shadowgraphs can be used to obtain qualitative and quantitative information about wake geometry, wake/body interactions, and blade/vortex interactions in forward flight. Video cameras were used for the first time to record the shadowgraphs. These provided several advantages compared to still cameras, and greatly enhance the capabilities of the shadowgraph method.

## Notation

- $A$  = rotor disk area,  $\pi R^2$ ,  $m^2$
- $c$  = blade chord,  $m$
- $C_T$  = rotor thrust coefficient,  $T/\rho A V_{tip}^2$
- $B$  = number of blades
- $R$  = rotor radius,  $m$
- $T$  = rotor thrust,  $N$
- $V_{tip}$  = rotor tip speed,  $\Omega R$ ,  $m/s$
- $V_\infty$  = free stream wind speed,  $m/s$
- $x$  = longitudinal distance from rotor centerline, parallel to free stream,  $m$
- $y$  = vertical distance from blade tip, perpendicular to free stream,  $m$
- $\mu$  = rotor advance ratio,  $V_\infty/\Omega R$
- $\rho$  = air density,  $kg/m^3$
- $C_N$  = rotor solidity coefficient,  $Nc/\pi R$
- $\Omega$  = rotor rotational speed,  $rad/sec$

## Introduction

The wake geometry of a helicopter determines many aspects of helicopter performance in forward flight. Knowledge of the overall wake geometry is vital for accurately calculating the performance and dynamics of the rotor. Understanding the interaction between the tip vortex and the fuselage is important for the analysis of aircraft performance and vibratory loads. While knowledge of the close interaction between the trailed

tip vortices and the blade (blade/vortex interaction) is important for airload prediction and for the study of acoustics. This paper examines the usefulness of the wide-field shadowgraph technique for studying each of these areas.

Research has been conducted to experimentally quantify the wake geometry for a helicopter in forward flight. In early work, Lehman tracked vortex trajectories from a model rotor in a water tunnel (Ref. 1). Biggers *et al.* (Ref. 2) used a laser velocimeter to quantify tip vortex locations over a limited portion of the rotor disk. Tangler (Ref. 3) used the schlieren method to examine blade/vortex interactions for small-scale rotors in descent and in high-speed flight. Landgrebe *et al.* (Ref. 4) used both schlieren and smoke-flow visualization to obtain the most complete forward-flight data to date. Recently, Brand *et al.* (Ref. 5) used a laser light sheet to examine wake/body interactions in low-speed forward flight. They examined a large number of individual cross sections of the flow to determine tip vortex trajectories.

The wide-field shadowgraph method has been a useful tool for examining tip vortex geometry for hovering rotors (Refs. 6–8) but its application to forward flight has not been extensively examined. This technique offers several advantages over the other methods mentioned; it does not require special models or seeding of the flow, and it is relatively simple to set up and operate.

The wide-field shadowgraph technique was first used to examine helicopter tip vortex location in forward flight in a joint Army/NASA/Boeing small-scale test at the Duits Nederlandse Wind tunnel (DNW) (Ref. 8). This test used a 1/5-scale Boeing Model 360 rotor. Shadowgraphs from this test were obtained

only from below the rotor on the advancing side and showed the convection of the wake as it progressed downstream at low advance ratios.

A test was recently conducted by NASA to more fully determine the usefulness of the wide-field shadowgraph technique for examining wake phenomena of a model helicopter rotor in forward flight. In this test, the wake was more completely examined than in the earlier forward-flight shadowgraph test. This was accomplished by obtaining side- and top-view shadowgraphs for all four quadrants of the rotor. The visibility of the tip vortices in the shadowgraphs was examined for a wide variety of rotor operating conditions. The use of videotape as a recording medium for the shadowgraphs was also examined.

This paper presents representative results from the test. These results include shadowgraphs for several run conditions and quantitative data obtained from the shadowgraphs.

### Test Setup

The test was conducted at the Glenn L. Martin Wind Tunnel at the University of Maryland. This wind tunnel has a test section of  $2.36 \times 3.35$  m. The rotor used in the test was a 1.651 m-diameter, four-bladed, fully articulated rotor. The blades had a constant chord and rectangular tips. Rotor characteristics are summarized in Table 1. The fuselage was a body of revolution that approximated a helicopter (main body and tail boom) configuration (Ref. 9). The rotor and fuselage are shown installed in the tunnel in Fig. 1.

The shadowgraph system consists of a camera; a short duration, high-intensity, point-source strobe; and a retroreflective screen (Fig. 2). Shadows of the rotor tip vortices are cast on the screen when the light passes through the rotor wake. These shadows are the result of changes in the refractive index of the air caused by the naturally occurring density gradients in the tip vortex core. The light is then reflected from the retroreflective screen back to the camera, producing an image with thin, dark curves that are projections of the tip vortices.

For this test, the windows of the wind tunnel test section were replaced with plywood sheets. Holes were cut in the plywood to provide a clear optical path for the strobe and camera. The shadowgraph screens are visible on the floor and the side wall in Fig. 1.

Shadowgraphs of the entire rotor system could not be obtained with this test setup because of the short distance between

Table 1 Rotor characteristics

Number of blades	4
Rotor radius	0.8255 m
Blade chord	0.0635 m
Rotor solidity	0.098
Blade twist (linear)	-12°
Airfoils	NASA RC(3), RC(4) Series

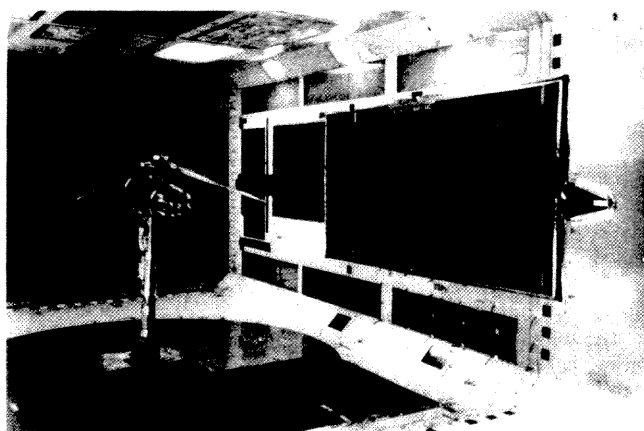


Fig. 1 Model setup for shadowgraph test in the wind tunnel.

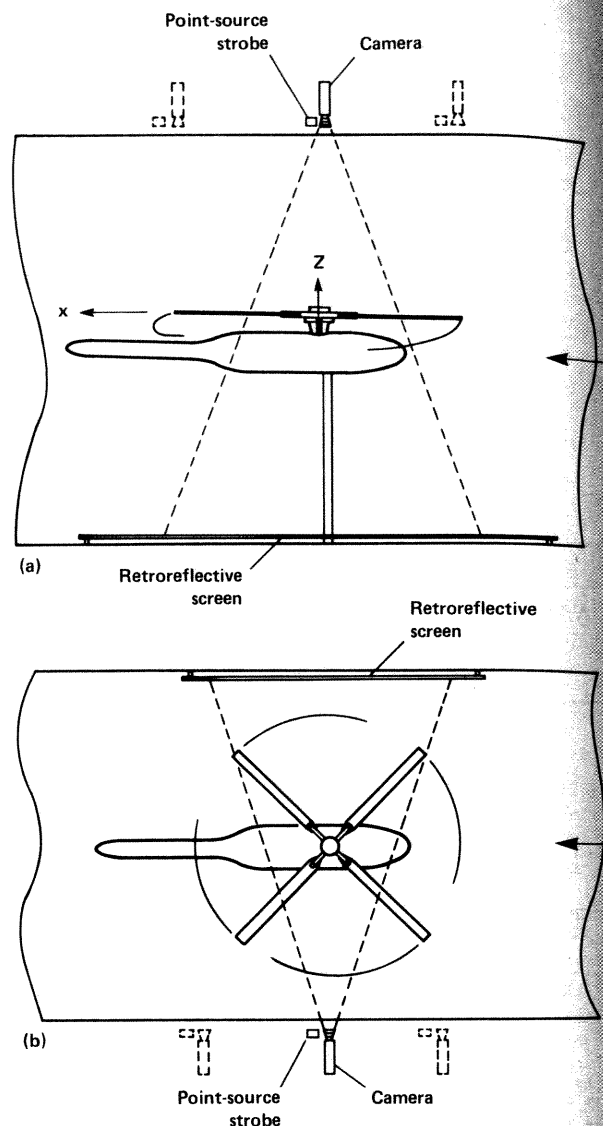


Fig. 2 Setup of shadowgraph system in the wind tunnel.

the camera and screen. Consequently, camera locations were selected to record large portions of the wake with the intent of compiling results from similar run conditions after the test. These camera locations provided both top and side views of the rotor wake. For the top-view shadowgraphs, cameras were placed above the rotor in one of four quadrants (Fig. 3). The side-view photos were obtained using one of three camera locations: upstream, rotor centerline, and downstream (Fig. 3). (The camera locations are also shown in Fig. 2.) Shadowgraphs were obtained using a 70 mm still camera and a VHS video camera.

Runs were conducted at 1800 and 1860 rpm, corresponding to a tip Mach number of 0.45 to 0.46. Advance ratios were varied from 0.00 to 0.175, and  $C_T/\sigma$  from 0.02 to 0.10. All runs were conducted with the rotor shaft tilted 6 deg forward.

### Sample Shadowgraphs

Examples of the shadowgraphs acquired during this test are shown in Figs. 4-6. The free-stream velocity in all shadowgraphs presented in this paper travels from right to left. Figure 4 shows a side-view shadowgraph taken from the front of the rotor. The schematic in the figure shows the rotor blade orientation and the blade numbering scheme. The blade visible

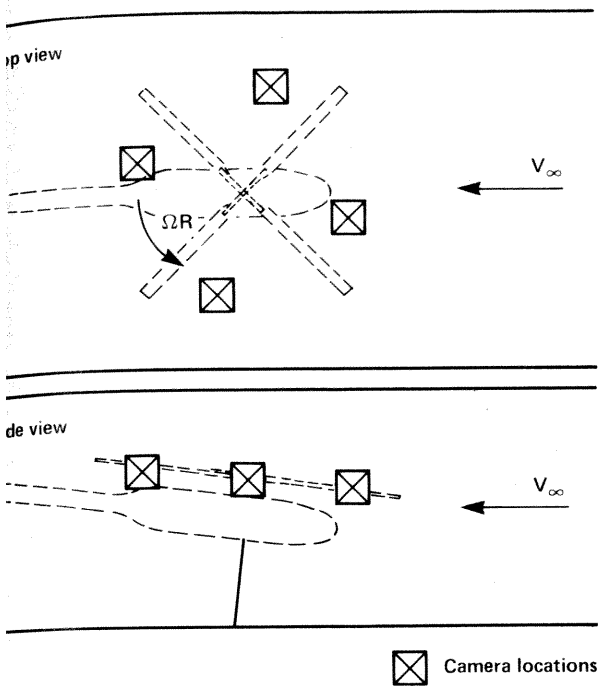


Fig. 3 Camera and strobe locations.

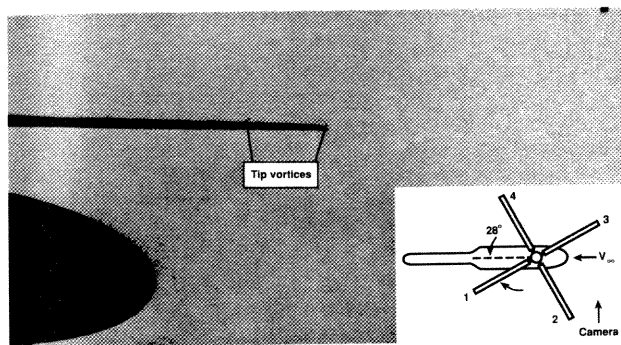


Fig. 4 Side view of rotor, upstream ( $C_T/\sigma = 0.09$ ,  $\mu = 0.075$ ).

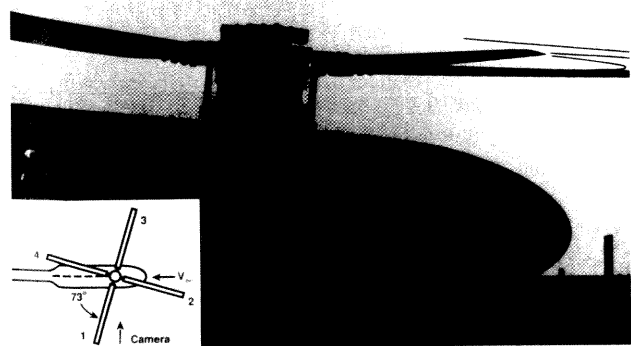


Fig. 5 Side view of rotor, at rotor centerline ( $C_T/\sigma = 0.09$ ,  $\mu = 0$ ).

this figure is blade 3. The tip vortex from blade 3 trails from blade tip. The tip vortex of blade 4 is visible downstream the tip of blade 3. The upwash at the front of the rotor disk apparent since the tip vortex of blade 4 has convected above the disk. Figure 5 shows a side-view shadowgraph taken at the rotor centerline. This shadowgraph has been enhanced to make the

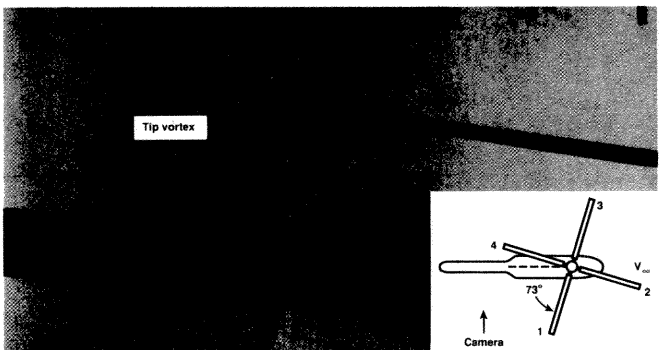


Fig. 6 Side view of rotor, downstream ( $C_T/\sigma = 0.09$ ,  $\mu = 0.075$ ).

tip vortices visible after publication. Two tip vortices are visible on the forward part of the rotor. The amount of wake information available from this view is limited in two ways. First, the tip vortices are hidden in areas where the blades block the light from the strobe. This problem could be reduced if the camera were placed slightly above the tip path plane to minimize the blade blockage of the tip vortices. A second limitation of this view is the low visibility of the tip vortices. The outer edges of the rotor wake are not captured well in this view, and as observed in previous tests, the outer edge of the rotor wake is the tip vortex's most visible section. This varying visibility of the tip vortex in any view is an inherent limitation of the shadowgraph technique. At the outer edge of the rotor wake, the tip vortex is parallel to the light path. This provides a long path length for the refraction of the light, and thus a dark image. Toward the center of the rotor wake, the light path is approximately perpendicular to the tip vortex. Therefore, refraction occurs only over a short path, with a length on the order of the vortex core diameter. Segments of the tip vortex in this region will produce a relatively faint image. The downstream half of the rotor system is shown in the shadowgraph of Fig. 6. This shadowgraph shows blade 4 and the fuselage along with the tip vortex. The tip vortex visible in the figure is from blade 1. This figure shows the tip vortex convecting downstream and traveling down from the rotor disk.

Shadowgraph Visibility

One objective of this test was to document the operating conditions for which tip vortices are visible when using the wide-field shadowgraph technique. These visibility conditions are shown graphically in Fig. 7 for side-view shadowgraphs. The visibility of tip vortices with the shadowgraph technique has been plotted as a function of both  $C_T/\sigma$  and advance ratio. The dotted line defines the approximate boundary of operating conditions where shadowgraphs were visible for this test. For low advance ratios ( $\mu = 0.05$ ), the tip vortices are visible for  $C_T/\sigma$  as low as 0.05. However, the vortex visibility decreases at higher advance ratios so that  $C_T/\sigma = 0.09$  is required for vortex visibility at  $\mu = 0.175$ .

At low advance ratios, large segments of the tip vortex geometry are often visible, as seen in Figs. 4 and 6. However, at higher advance ratios this visibility decreases, with only the edge of the rotor wake remaining visible. Two to three tip vortices are visible for the rotor at advance ratios up to 0.15, but with increasing speed, less of each vortex is visible.

The top-view shadowgraphs do not provide the high tip vortex visibility found in the side-view shadowgraphs. This is thought to be caused by the fact that the tip vortices are perpendicular to the light path, as discussed above. However, some tip vortices are visible. A shadowgraph obtained from the top of the rotor at the forward camera location is presented in Fig. 8. The tip vortices are faint and have been enhanced in this figure for clarity. Two trailed vortices are visible. The visibility of the top-view shadowgraphs obtained in this test is significantly less

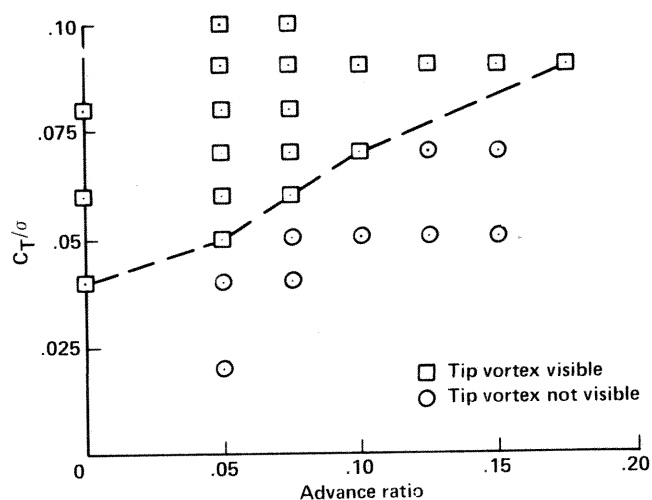
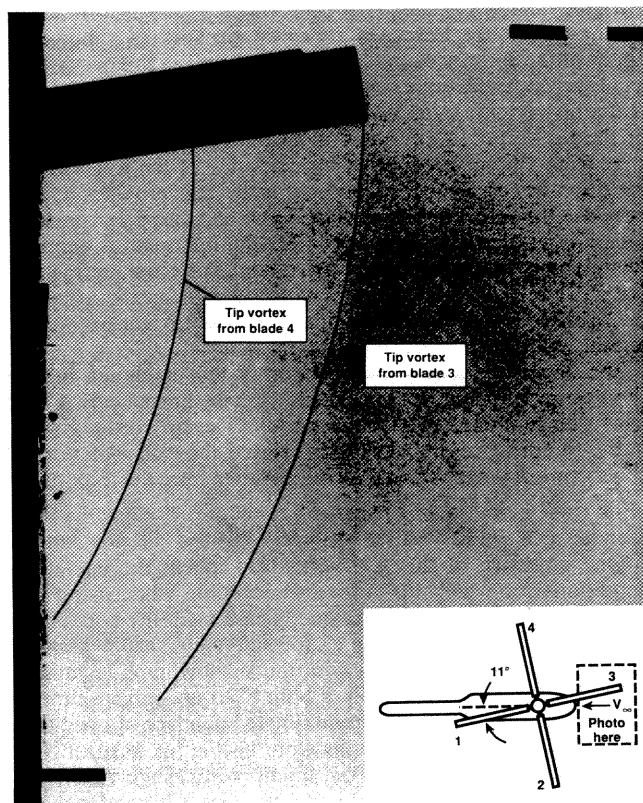


Fig. 7 Shadowgraph visibility.

Fig. 8 Top view of rotor, forward camera location, ( $C_T/\sigma = 0.09$ ,  $\mu = 0.075$ ).

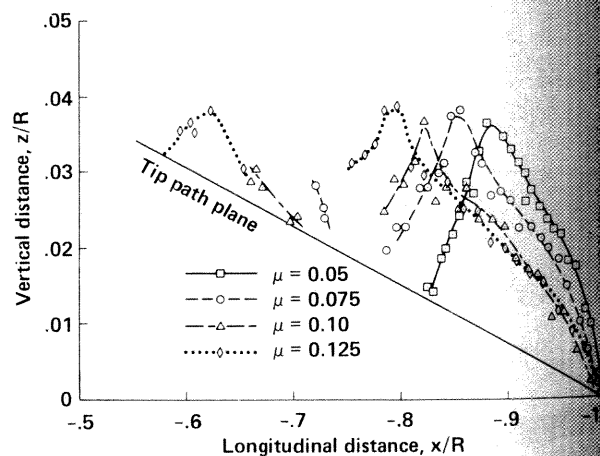
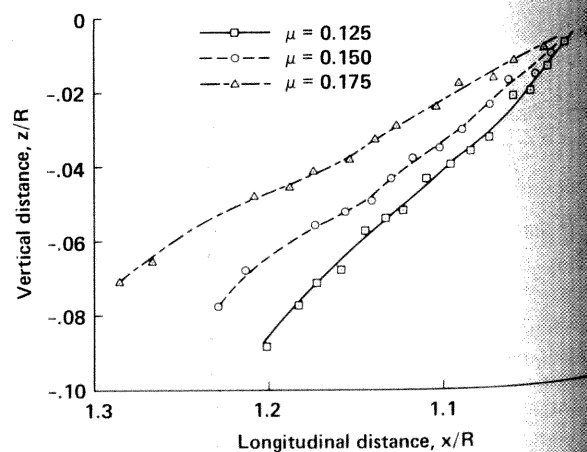
than that found in the forward-flight test cited in Ref. 8. The reason for this is not currently understood.

Previous work on shadowgraph visibility (Ref. 6) indicated that the tip vortex visibility should significantly increase on the retreating side of the rotor in forward flight, when compared to the advancing side. After examining the shadowgraphs obtained in this test, no significant difference in visibility was found. This finding, however, is not conclusive because of the relatively poor visibility of all top-view shadowgraphs obtained during the present test. Further research is required to understand this more completely.

### Wake Geometry in Forward Flight

The wide-field shadowgraph technique is useful for examining the wake geometry of a helicopter in forward flight. As an example of this, two-dimensional wake data were obtained from the side-view shadowgraphs acquired during this test. A sequence of shadowgraphs taken at different blade azimuth settings was examined, and the resulting wake boundaries were determined. The final reduced data are shown in Fig. 9. The coordinate system for these plots is defined in Fig. 2. Each data point in the figure represents an  $\sim 6$  deg increment in rotor blade azimuth, so the figure essentially shows how the location of the tip vortex at the edge of the rotor wake changes with time. Figure 9a shows the wake boundaries for the front of the rotor. The approximate location of the rotor tip path plane is included in the figure for reference. The wake travels above the rotor and downstream, as noted in Ref. 4. As expected, increasing the advance ratio causes the tip vortex to move downstream faster. The peak in each curve corresponds to the passage of the following blade. This blade passage induces the tip vortex downward. The maximum distance of the tip vortex above the rotor decreases with increasing advance ratio. Also, the downstream location of this maximum increases with advance ratio. The gaps in the data at higher  $x/R$  are caused by the blade blocking the shadowgraph. The data for  $x/R > -0.1$  show the wake boundary moving away from the blade. This is caused by the close blade/vortex interaction at the second blade passage.

Figure 9b shows the wake boundaries for the rear of the rotor. This figure shows the downward and aft travel of the

Fig. 9a Measured wake boundaries, front of rotor ( $C_T/\sigma = 0.09$ ).Fig. 9b Measured wake boundaries, rear of rotor ( $C_T/\sigma = 0.09$ ).



ke for increasing advance ratios. Note that the blade passage has no noticeable effect on the vortex position for these advance ratios.

The data set in Fig. 9 is an example of the quantitative information obtainable using the wide-field shadowgraph technique. A comprehensive test program would more completely define the wake geometry for a variety of operating conditions and could provide data for comparisons with analytical work. More complete wake geometry data can be obtained by combining simultaneously obtained side- and top-view shadowgraphs to give three-dimensional information on the wake geometry in forward flight. The methodology required to obtain such three-dimensional wake geometry data from simultaneous shadowgraphs is currently being developed.

Wake/Body Interactions

In addition to overall wake geometry data, the wide-field shadowgraph technique can be used to look at specific physical aerodynamic phenomena, including wake/body interactions, as noted in Ref. 6. One example of this from the current test is the interaction between the fuselage and wake in low-speed forward flight, as shown in Fig. 10. Three tip vortices are visible in this figure, two above the fuselage and one below. The first visible tip vortex has an undistorted, helical trajectory, while the next lower tip vortex is distorted near the fuselage. This distortion shows the reduced local tip-vortex descent rate resulting from the fuselage blockage of the wake.

A third tip vortex is visible below the fuselage. Unfortunately, the mechanism by which the tip vortex passes over the fuselage is not discernible. The fact that the tip vortex visibility ceases downstream suggests that the strength of the tip vortex decreases. Whether this is through stretching, bursting, or instability is not currently understood.

By taking shadowgraphs at different blade azimuth locations, the tip vortex can be traced down the length of the fuselage. These shadowgraphs indicate that the vortex wraps around the fuselage as it convects downstream. More work is required to accurately define the process of the tip vortex interaction with the fuselage. One possible approach is to apply reflective sheeting to the fuselage in addition to the wall behind the rotor.

Wake/body interactions are also visible from the top view. Figure 11 shows a shadowgraph obtained from the rear top-view camera location. The figure has been enhanced to show the faint tip vortices. The tip vortex from blade 2 stretches downstream directly over the fuselage. This suggests an accelerated streamwise flow over the fuselage at this location. These results indicate the type of wake/body interaction information that can be obtained using the wide-field shadowgraph technique. Since the best shadowgraph results were obtained at low advance ratios, use of the wide-field shadowgraph technique is ideally suited for examining low-speed

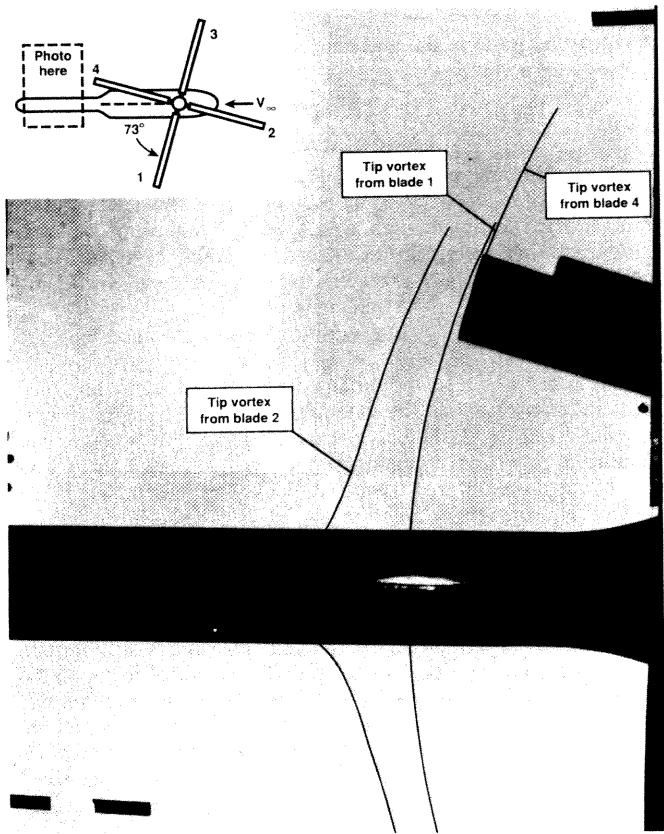


Fig. 11 Wake/body interaction, top view ( $C_T/\sigma = 0.09$ ,  $\mu = 0.05$ ).

wake/body interactions. Future work is needed to quantify the changes in tip vortex geometry caused by a fuselage and should help to understand the mechanism by which the tip vortex passes over the fuselage.

Blade/Vortex Interactions

Another specific phenomenon which can be studied with the wide-field shadowgraph technique is the interaction between a blade and a vortex. The digitized video image of the shadowgraph in Fig. 12 shows a perpendicular blade/vortex interaction on the forward part of the rotor. The figure shows the interaction between blade 2 and the tip vortex from blade 4. By combining side-view shadowgraphs such as this with simultaneous top-view shadowgraphs, it would be possible to

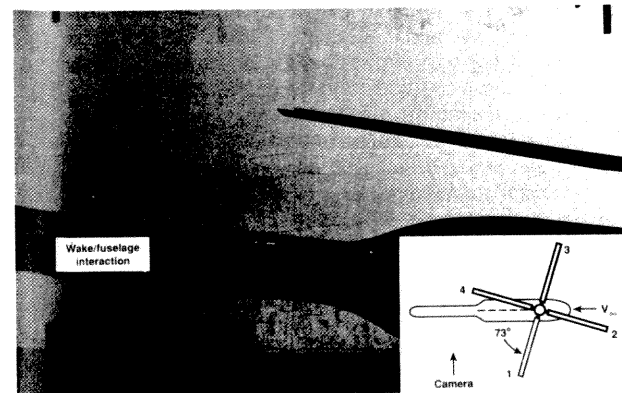


Fig. 10 Wake/body interaction, side view ( $C_T/\sigma = 0.09$ ,  $\mu = 0.05$ ).

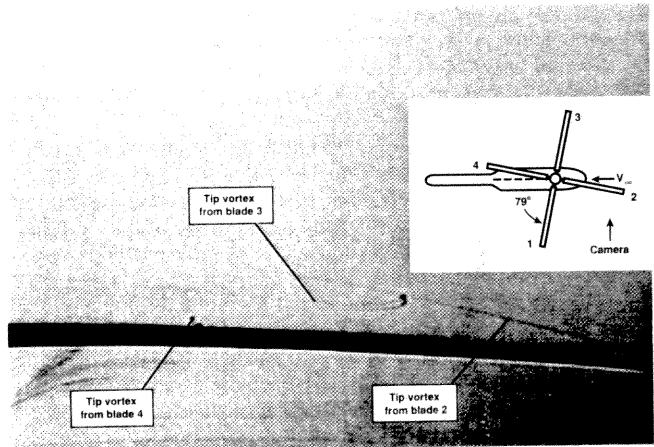


Fig. 12 Blade/vortex interaction ( $C_T/\sigma = 0.09$ ,  $\mu = 0.075$ ).

quantify both the radial and azimuthal locations of this blade/vortex interaction.

### Video Capabilities

One additional objective of the test was to determine the feasibility of using video as an imaging device. To accomplish this, a VHS video camera was used for recording the shadowgraph data in hover and in forward flight. In general, excellent shadowgraphs were achieved from the side view using video, while poor tip vortex visibility was obtained from the top view. This is consistent with the results obtained with the still camera.

The rotor speed was maintained at 1800 rpm for the video runs in order to match the video frame rate with the once-per-revolution strobe flash. This essentially provided a stop-motion picture at a particular blade azimuth location. The steadiness of the tip vortices in forward flight was apparent using the video. The tip vortex location varied very little, if at all, for the first two vortices. However, by the third blade passage unsteadiness was noticeable, and unsteadiness also increased at the higher advance ratios.

As a result of this testing, it is clear that the video camera solves some of the problems inherent in using a still camera for taking shadowgraphs. First, it gives instant feedback on the quality of the shadowgraphs since no processing is required. The researcher can immediately tell if the tip vortices are visible at the current operating conditions and if the shadowgraph parameters (camera aperture setting, strobe intensity) are properly adjusted. Second, the video camera provides the researcher with a means of examining different areas of the flow field. The ability to pan and zoom over the entire flow field allows the researcher to carefully examine areas of particular interest. Many of the observations reported in this paper were first identified with the video camera.

It is possible to digitize frames from a live camera or videotape using present computational resources. These digitized video images allow increased automation of the data reduction process that is required to obtain quantitative data from the shadowgraphs.

One potential limitation of the video camera is the relative decrease in image resolution. The video setup used in this test provided only 220 lines of horizontal resolution, which is significantly lower than that available with still photographs. High resolution video imaging systems that are capable of being synchronized with the rotor and strobe frequencies will be used in future small- and large-scale testing.

### Conclusions

The wide-field shadowgraph technique has been used to examine the tip vortex geometry of a helicopter in forward flight. The results of the test showed the following:

- 1) The tip vortices are visible for advance ratios up to 0.17, provided the rotor thrust is high enough. In general, the best results are obtained at low advance ratios.
- 2) The wide-field shadowgraph method can provide information on forward-flight wake geometry, wake/body interactions, and blade/vortex interactions.
- 3) Video can be used to obtain shadowgraphs, and it provides more flexibility and faster results than still photography.

### Acknowledgments

The authors of this paper would like to thank Mr. Robert Wozniak and the entire staff at the Glenn L. Martin Wind Tunnel for their invaluable assistance in conducting this test.

### References

- <sup>1</sup>Lehman, A. F., "Model Studies of Helicopter Rotor Flow Patterns," American Helicopter Society 24th Annual Forum, Washington, D.C., May 1968.
- <sup>2</sup>Biggers, J. C., Lee, A., Orloff, K. L., and Lemmer, O. J., "Measurements of Helicopter Rotor Tip Vortices," American Helicopter Society 33rd Annual Forum, Washington, D.C., May 1977.
- <sup>3</sup>Tangler, J., "Schlieren and Noise Studies of Rotors in Forward Flight," American Helicopter Society 33rd Annual Forum, Washington, D.C., May 1977.
- <sup>4</sup>Landgrebe, A. J., Taylor, R. B., Egolf, T. A., and Bennett, J. C., "Helicopter Airflow and Wake Characteristics for Low Speed and Hovering Flight from Rocket Interference Investigations," American Helicopter Society 37th Annual Forum, New Orleans, La., May 1981.
- <sup>5</sup>Brand, A., Komerath, N., and McMahon, H., "Results from Laser Sheet Visualization of a Periodic Rotor Wake," AIAA Paper 88-0192, AIAA Aerospace Sciences Meeting, Reno, Nev., Jan 1988.
- <sup>6</sup>Norman, T., and Light, J., "Rotor Tip Vortex Geometry Measurements Using the Wide-Field Shadowgraph Technique," *Journal of the American Helicopter Society*, Vol. 32, (2), Apr 1987.
- <sup>7</sup>Light, J., "Tip Vortex Geometry of a Hovering Helicopter Rotor and Ground Effect," American Helicopter Society 45th Annual Forum, Boston, Mass., May 1989.
- <sup>8</sup>Norman, T., and Light, J., "Application of the Wide-Field Shadowgraph Technique to Rotor Wake Visualization," 15th European Rotorcraft Forum, Amsterdam, Sep 1989.
- <sup>9</sup>Leishman, J. G., Bi, N., Samak, D. K., and Green, M., "Investigation of Aerodynamic Interactions Between a Rotor and a Fuselage in Forward Flight," American Helicopter Society 45th Annual Forum, Boston, Mass., May 1989.